CHAPTER IV
RESULTS AND DISCUSSION

4.1 Monomer Preparation

The effect of solvent on the synthesis of diamine-based benzoxazine was studied by comparing between the melt method and the solvent method.

Table 4.1 Monomer synthesis conditions

Solvent	Temperature (°C)	Reflux Time (min)	Products
Solventless	80	30	Sudden polymerization yielding oligomers and polymer, no monomer was obtained.
Solventless	40/ 80	30/ 30	Oligomers were obtained.
Solventless	30	30	5% yield of white solid monomer
Solventless	30	10	7% yield of white solid monomer
Toluene	110	240	Monomer and some oligomers were obtained as a pale-yellow viscous fluid.
$CHCl_3$	60	90*	60% yield of white solid monomer
CH_2Cl_2	40	120*	61% yield of white solid monomer.

* The reaction time for the highest percent yield.

From the solvent method, both chloroform and dichloromethane, which have lower reflux temperatures, yielded more monomer than toluene, which has higher reflux temperature. Due to the exothermic reaction, using solvent and lower temperature gave higher yields.

In the solventless method, several temperature programs were used (Table 4.1), but all of them gave almost the same results, the reactants immediately underwent the Mannich condensation reaction and ring-opening polymerization.

Oligomers were obtained instead of the monomers because the reaction heat generated made the reaction temperature go up leading to the ring opening of the monomers. Compared with the dilute system, the solvent helped heat dissipation better than that of the solventless system so greater amount of monomer was obtained. This is in contrast to the lesser reactive aromatic amines where high yield was obtained with the solventless method (H. Ishida, U.S. Pat. 5,543,516, Aug. 6 (1996)).

4.2 Monomer Characterization

The FTIR spectrum of the bifunctional benzoxazine monomer is shown in Figure 4.1. The bands that appear in the frequency region 1550-1400 cm^{-1} are due to the substituted benzene ring. The bands in the region 1240-1210 cm^{-1} and 1040-1020 cm^{-1} correspond to the antisymmetric and symmetric C-O-C stretching modes. The region of 1150-1050 cm^{-1} is due to the C-N-C antisymmetric stretching, while the symmetric stretching mode appears at 800-720 cm^{-1}. Another characteristic band is the absorption at 918 cm^{-1} which is assigned to the C-H out-of-plane deformation (Rodriguez, 1995).

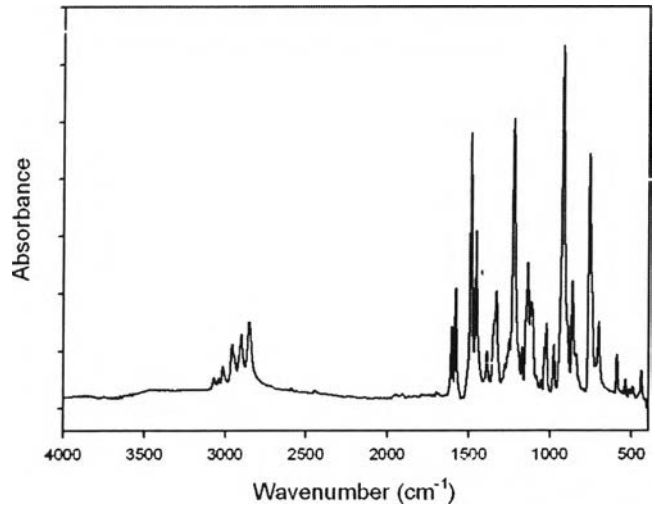

Figure 4.1 FTIR spectra of the diamine-based benzoxazine monomer.

Inspection of the ^{1}H NMR spectrum of the diamine-based monomer reveals three resonances at respective chemical shifts of 4.9, 4.1 and 3.0 ppm with equal integrated intensities (Figure 4.2). This implies that three different methylene groups exist in the structure. The singlet peaks at 4.9 and 4.1 ppm are the signal of methylene units in the oxazine ring and the other singlet peak at 3.0 ppm corresponds to the methylene bridge linking the two oxazine rings. The aromatic protons show multiplets around 7.5-8.5 ppm. The intensity integration confirms the difunctional structure of the diamine-based benzoxazine monomer. Along with the lack of small resonances in this area, which is the case when synthesis impurities are present, the monomer obtained was of very high purity.

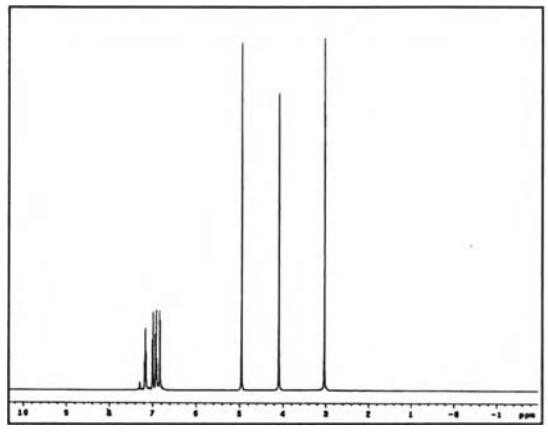

Figure 4.2 ^{1}H NMR spectra of the diamine-based benzoxazine.

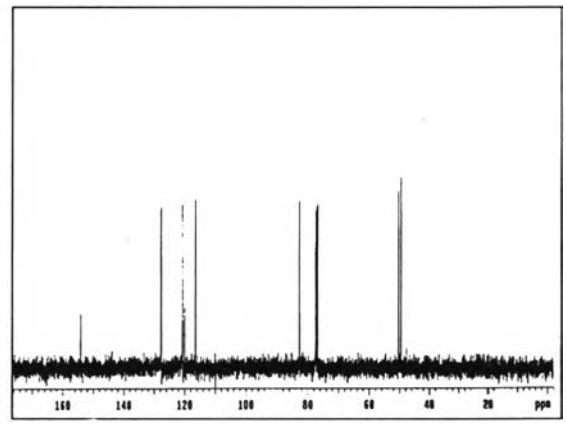

Figure 4.3 ^{13}C NMR spectra of the diamine-based benzoxazine.

In addition to ^{1}H NMR analysis, ^{13}C NMR has also been utilized to determine the structure of the monomer (Figure 4.3). The resonance peaks at 82 and 51 ppm are assigned to the aliphatic methylene carbons in the oxazine ring and the resonance at 49 ppm is assigned to the methylene carbons of the bridge linking the two oxazine rings. The aromatic carbons show the resonance peak between 110 and 160 ppm.

Thermal characterization of the benzoxazine was accomplished by TGA and DSC. The result of the TGA experiment is shown in Figure 4.4. It can be seen that the polybenzoxazine remained stable up to 240°C with the char yield at 800°C under nitrogen of 41%.

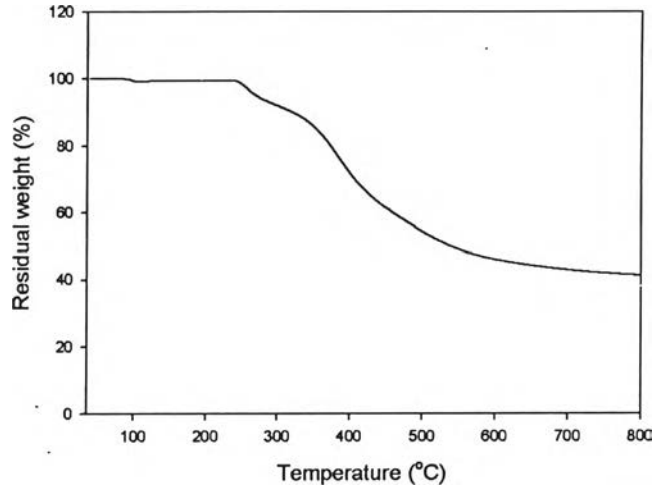

Figure 4.4 TGA thermogram of the diamined-based benzoxazine monomer.

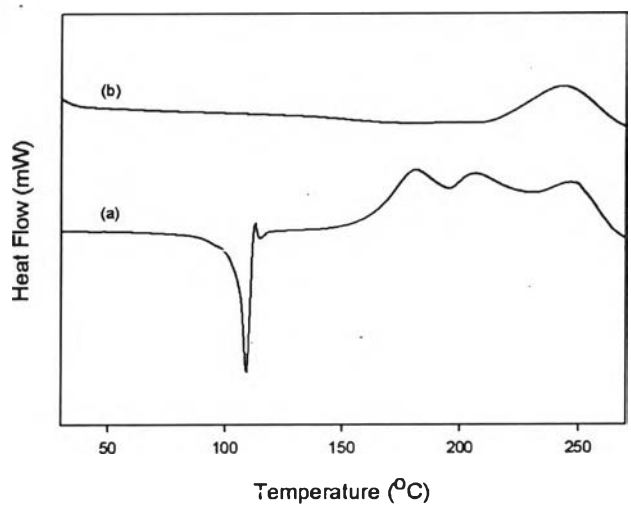

Figure 4.5 DSC thermograms of (a) the diamined-based benzoxazine monomer and (b) the polybenzoxazine cured at 180 °C for 1 hour and 200 °C for 30 minutes.

The non-isothermal DSC thermograms of bifunctional benzoxazine are presented in Figure 4.5. There is a melting endotherm at 113°C. Multiple exotherms centered at 180, 207, and 249°C, respectively, are also seen. The two low temperature exotherms might be due to the polymerization of benzoxazine resin (D.J. Allen and H. Ishida, Polymer (submitted)). The exotherm at 249°C is due to the degradation rather than further curing as shown by the TGA experiment indicating that degradation begins at about 240°C. This peak was also observed in the DSC

curve of the fully thermally polymerized polybenzoxazine (Figure 4.5b). The glass transition temperature of the polybenzoxazine is about 160°C as determined from the very weak transition in the same thermogram.

4.3 Fiber Surface Treatment

4.3.1 Alkali Treatment

The alkali treatment promotes the partial removal of the hemicellulose, wax, and lignin present on the fiber surface (Aziz, 2004) leading to changes in fiber morphology and chemical composition. The change in the surface morphology of the treated fibers was studied by Scanning Electron Microscope (SEM).

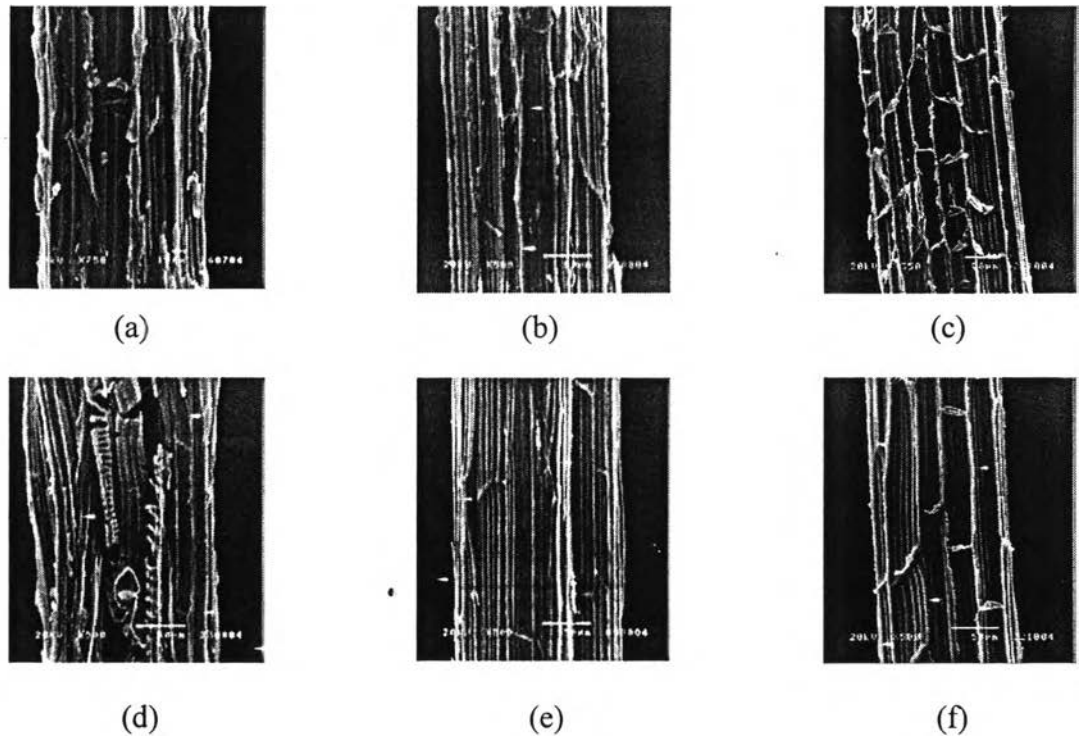

Figure 4.6 SEM micrographs of (a) the untreated sisal, (b) γ–APS treated sisal, (c) γ–GPS treated sisal, (d) NaOH treated sisal, (e) NaOH/γ–APS treated sisal, (f) NaOH/γ–GPS treated sisal.

From Figure 4.6, it can be seen that the alkali treated fiber has a rougher surface and more crevices on the surface than the untreated one. Besides, some loosely spiraled fibrils are exposed indicating that some cementing materials in fibers are removed. Figure 4.6 also shows the silane-treated fibers, which will be discussed in a later section.

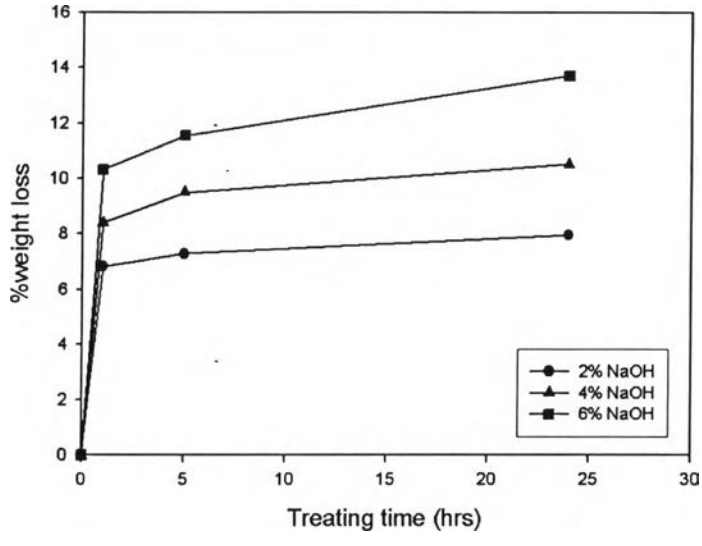

Figure 4.7 Percent weight loss of sisal fibers after NaOH treatment at different times.

The effect of alkali treatment on the amount of weight loss of fibers was studied at different concentrations of NaOH solution and times of treatment. Figure 4.7 shows that %weight loss of sisal fibers increases with NaOH concentration. The %weight loss was high initially followed by a more gradual weight loss at longer treatment time. In agreement with other lignocellulosic fibers, the significant weight loss of sisal fiber after alkali treatment can be ascribed to the partial dissolution of hemicellulose (Rong, 2001; Dansiri, 2002).

Figure 4.8 and 4.9 show FTIR spectra of untreated and NaOH treated sisal fibers. It can be seen that the intensity of the carbonyl stretching peak at 1730 cm^{-1} corresponding to hemicellulose of fibers (Rong, 2001) was continuously reduced when treating time and NaOH concentration increased until it can no longer be perceived for the 5 hours curve in Figure 4.8 and 6% curve in Figure 4.9. The 6% concentration and 5 hour-treating, in which hemicellulose at fiber surface was mostly

removed, were chosen to be the conditions of NaOH treatment for the next experimental part.

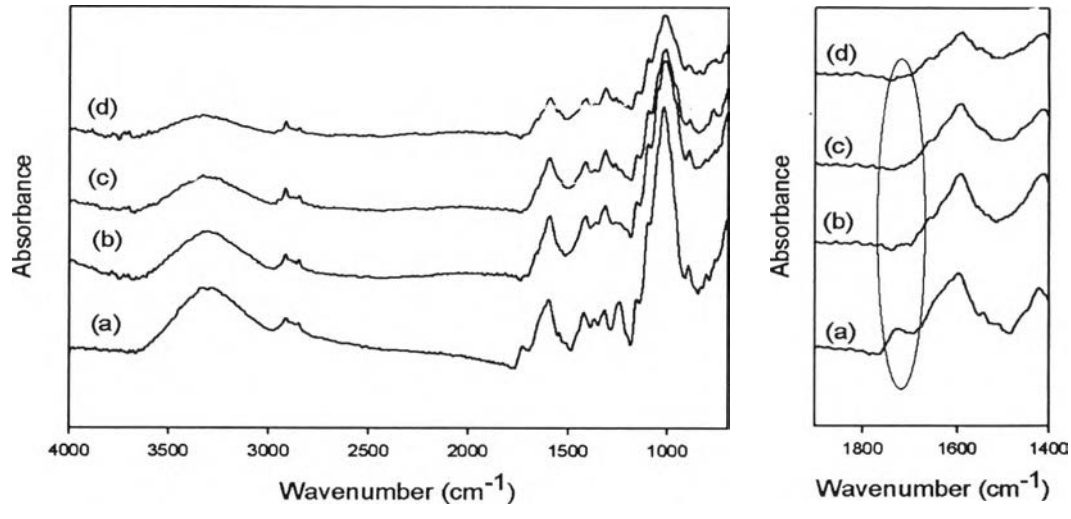

Figure 4.8 FTIR spectra of untreated fibers (a) and NaOH treated fibers with treating times of (b) 1 h, (c) 5h and (d) 24 h.

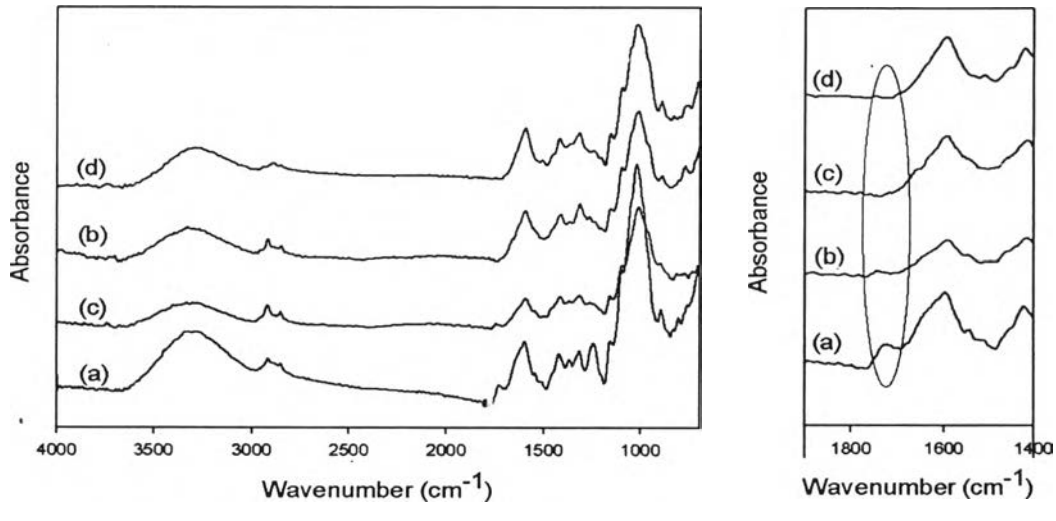

Figure 4.9 FTIR spectra of untreated fibers (a) and NaOH treated fibers at different concentrations of (b) 2%, (c) 4% and (d) 6%.

Figure 4.10 shows the TGA and DTG thermograms of untreated fibers and the fibers treated by 6% NaOH for 5 hours. The thermograms of untreated fibers shows two decomposition steps. The first peak appears at 300°C and corresponds to

the thermal decomposition of hemicellulose and the glycosidic links of cellulose. The second one appears at around 360°C due to the thermal decomposition of α–cellulose (Alvarez, 2004). In the case of NaOH treated fibers, the peak at 300°C is not present, while the whole TGA thermogram is shifted to higher temperature with a higher char yield indicating that the NaOH treated fibers are more thermally resistant.

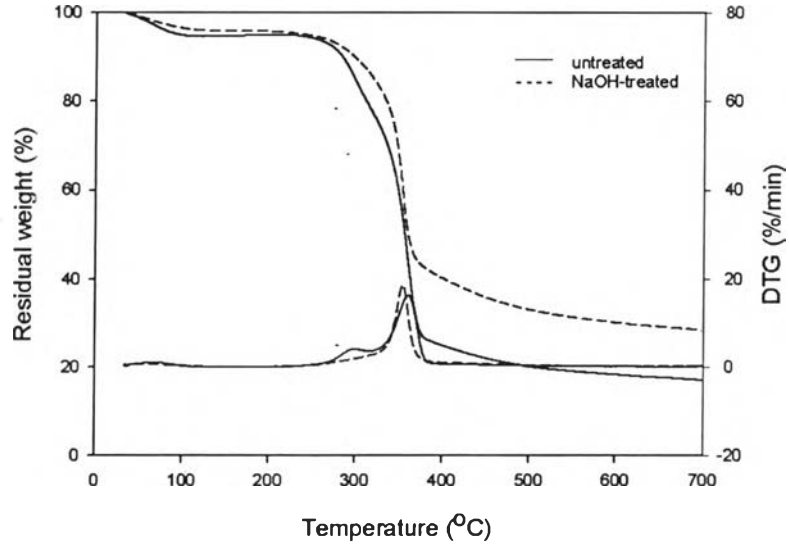

Figure 4.10 Thermograms of untreated fibers and the fibers treated by 6% NaOH for 5 hours.

4.3.2 Silane Treatment

SEM micrographs of the γ–aminopropyltrimethoxysilane (γ-APS)-treated fiber and the γ–glycidoxypropyltrimethoxysilane (γ–GPS)-treated fiber were shown in Figure 4.6. There is no dramatic change in the surface morphology of the silane treated fiber compared to the untreated one and the surface morphology of the NaOH/γ–APS treated and NaOH/γ–GPS treated fiber is also not visibly different from that of the NaOH treated fiber.

The FTIR using attenuated total reflection mode (ATR) was used to analyze the chemical functionalities present on the surface. Due to the small quantities of silanes present on the fiber surface, the analysis was based on the spectral differences between treated and untreated samples. The difference spectra of γ–APS and γ–GPS treated sisal surface are shown in Figure 4.12 and 4.13,

respectively. In general, free NH_2 groups show a band around 1600 cm^{-1}. From Figure 4.12, it can be seen that γ–APS treated fibers shows a distinctive absorbance peak at 1575 cm^{-1}. This band is the typical deformation mode of NH_2 groups hydrogen bonded to the OH functions of both silanol moieties and cellulosic fiber as shown in Figure 4.11 (Abdelmouleh, 2004; Plueddemann, 1982). The band around 1130 cm^{-1} is related to Si-O-C band while the absorption band at 1030 cm^{-1} corresponds to the Si-O-Si bonds (Abdelmouleh, 2004).

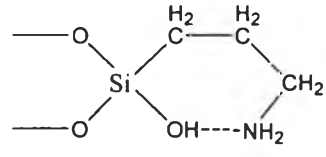

Figure 4.11 NH_2 group hydrogen bonded to the OH functions of silanol.

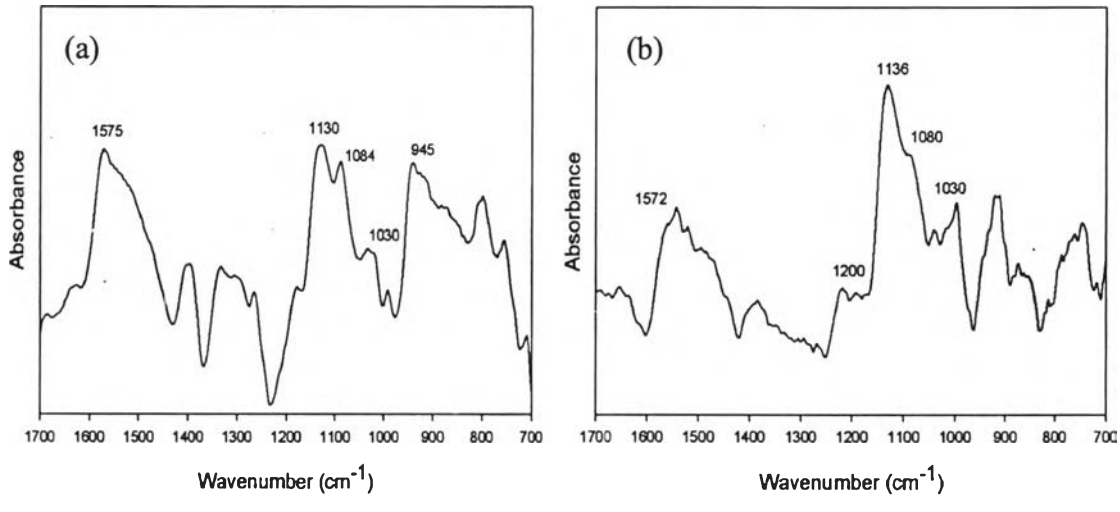

Figure 4.12 Difference spectra of (a) the γ–APS-treated and untreated fibers and (b) the NaOH/γ–APS treated and NaOH treated fibers.

The Si-O-Si bond is indicative of the existence of polysilsesquioxane deposited on the fiber and the Si-O-C bond would confirm the occurrence of a condensation reaction between the silane coupling agent and the sisal fiber. The Si-O-C group is also present in the unhydrolyzed silane. However, the conditions adopted in this study will not leave unhydrolyzed species to the detectable concentration. While the observation of the Si-O-C related band might seem to

indicate the presence of the interfacial bond, the weakness of the band and complex spectral features necessitate further study before conclusive statement can be made.

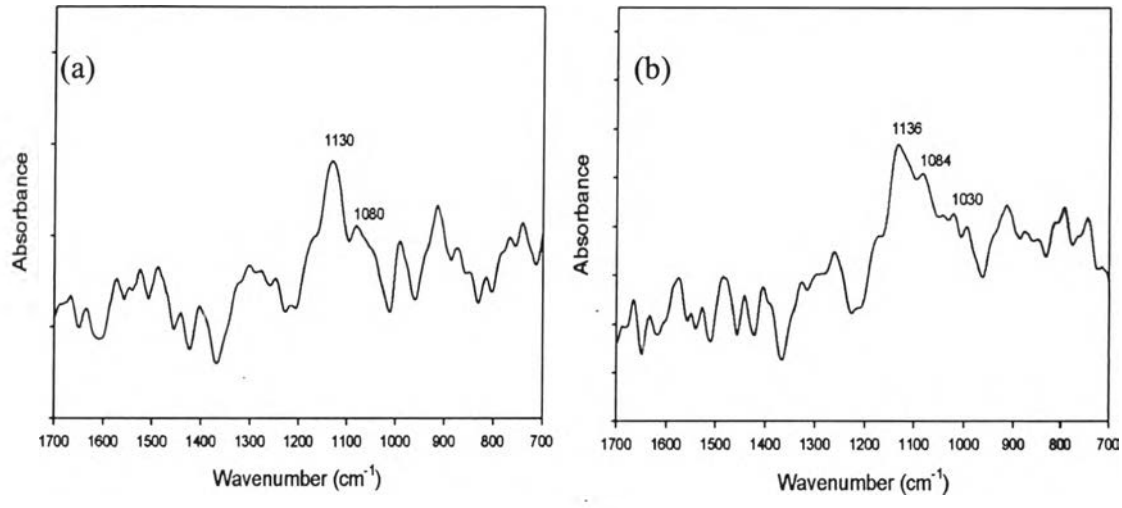

Figure 4.13 Difference spectra of (a) the γ–GPS-treated and untreated fibers and (b) the NaOH/γ–GPS treated and NaOH treated fibers.

The changes in the water contact angle on the sisal sheets after treatment with γ–APS, NaOH/ γ–APS, γ–GPS, and NaOH/ γ–GPS are shown in Figure 4.14, which represent the dynamic acquisition of the values of contact angle with time. With 0.1% γ–APS, the contact angle values increase from 62° to reach a high limit of about 72°. This increment results from the γ–APS configuration which is assumed to orient its polar NH_2 heads toward the fiber surface and form hydrogen bonds with the cellulose hydroxyl groups. Such configuration would leave the methylene sequence exposed at the surface, thus providing the hydrophobic character (Abdelmouleh, 2004). The higher concentration of γ–APS of 0.5% results in a higher limit of water contact angle of about 83°.

The NaOH treatment coupled with γ–APS treatment shows almost the same result as the treatment with only silane in the case of 0.1% γ–APS. However, in the case of 0.5% γ–APS treatment, the NaOH treatment enhances the hydrophobic character as can be seen from the highest value of contact angle at 89 °. From the results, it can be concluded that the alkali treatment removes some hemicellulose

from the fibers, thus making cellulose fibrils and their hydroxyl groups more exposed to the fiber surface. After alkali treatment, the condensation between the silanol groups of silane and the hydroxyl groups of the sisal fibers can occur more readily than that without alkali treatment.

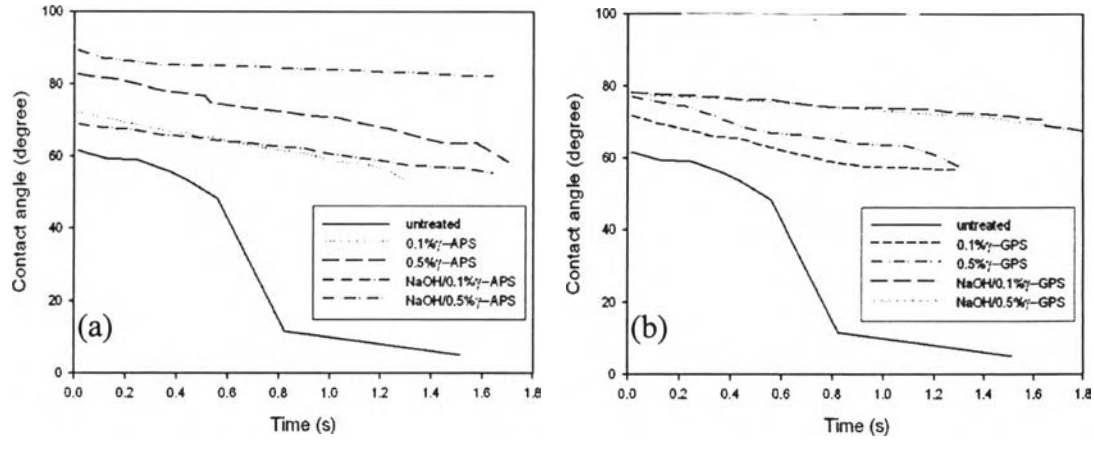

Figure 4.14 Water contact angle of untreated and treated sisal fibers; (a) amino-silane coupling agent (γ–APS) and (b) epoxy-silane coupling agent (γ–GPS).

In cases of γ–GPS, the contact angle increases from 62° to 72° with 0.1% γ–GPS and reaches a high limit of about 77° with 0.5% γ–GPS. As in the case of γ–APS, fibers treated by 0.1% and 0.5% γ–GPS after the alkaline treatment show the highest values of contact angle. From these results, it could be concluded that the silane was deposited on the fiber surface providing more hydrophobic character and the alkali treatment enhanced the efficiency of the deposition.

4.4 Composite Properties

4.4.1 Effect of Reinforcing Sisal Fibers

Sisal fibers were incorporated in a 50:50 benzoxazine:epoxy resin matrix to form a unidirectionally reinforced composite. The effect of reinforcing sisal fibers on mechanical properties was studied by varying percentage of sisal fiber of 5%, 10% and 15% by volume.

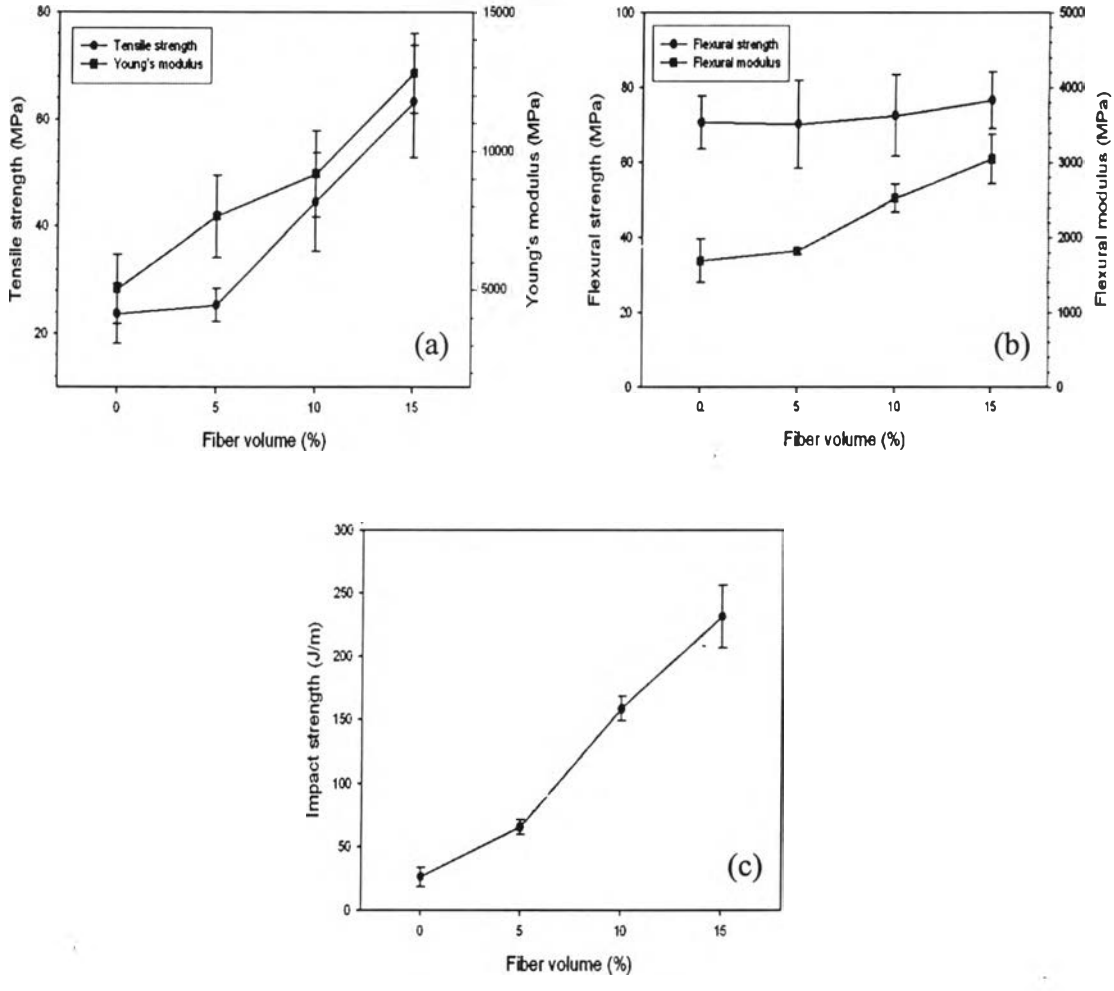

Figure 4.15 Effect of fiber volume on (a) tensile properties, (b) flexural properties, and (c) impact strength of sisal-benzoxazine/epoxy composites.

Figure 4.15 a, b and c show the comparison of mechanical properties of the benzoxazine/epoxy resin and sisal-benzoxazine/epoxy composites with various percents of fiber. The presence of sisal fibers leads to an increment of tensile strength and Young's modulus. The flexural properties slightly increased when sisal fibers were used as a reinforcing material. Besides, the impact strength was improved significantly in the sisal fiber reinforced benzoxazine/epoxy composites compared with benzoxazine/epoxy polymer. Thus, it can be concluded that the mechanical properties could be improved by incorporating sisal fibers in the benzoxazine/epoxy resin.

4.4.2 Effect of Matrix Composition

Benzoxazine-epoxy mixtures with 25%, 50%, 75% and 100% by weight epoxy were cured and incorporated with 10 vol% of sisal fibers for mechanical analysis. Anhydride and tertiary amine were used as a hardener and a catalyst to cure the 100% epoxy resin; however, the mixtures of benzoxazine-epoxy could be cured without them. The presence of epoxy resin significantly improves the processability of benzoxazine because the low viscosity of epoxy resin enhances fiber impregnation ability. Moreover, since the benzoxazine used still requires purification and degassing processes to eliminate any unreacted residues or solvent causing void formation in the curing step, the low viscosity epoxy resin helps to reduce the viscosity of the resin mixture making the entrapped air escape more easily.

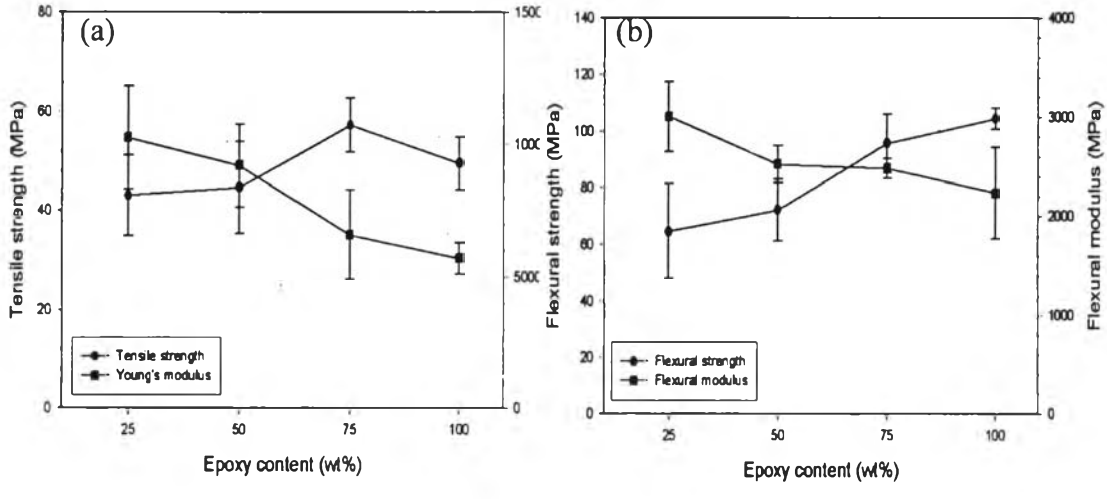

Figure 4.16 Dependence of (a) tensile properties and (b) flexural properties of sisal-benzoxazine/epoxy composites on the epoxy content in the resin mixture.

The tensile and flexural properties of the composites were determined as shown in Figure 4.16 (a) and (b). It can be seen that the tensile strength and flexural strength increase as the matrix becomes richer in epoxy content. The addition of epoxy may improve the perfection of the crosslinked network and contribute to the increased tensile strength and flexural strength. In contrast, the tensile modulus decreases with epoxy content or it can be stated that benzoxazine helps to increase the modulus of the composites. From Figure 4.17 (a), it is evident

that when we have high epoxy content, percent tensile strain at break of the composite increases.

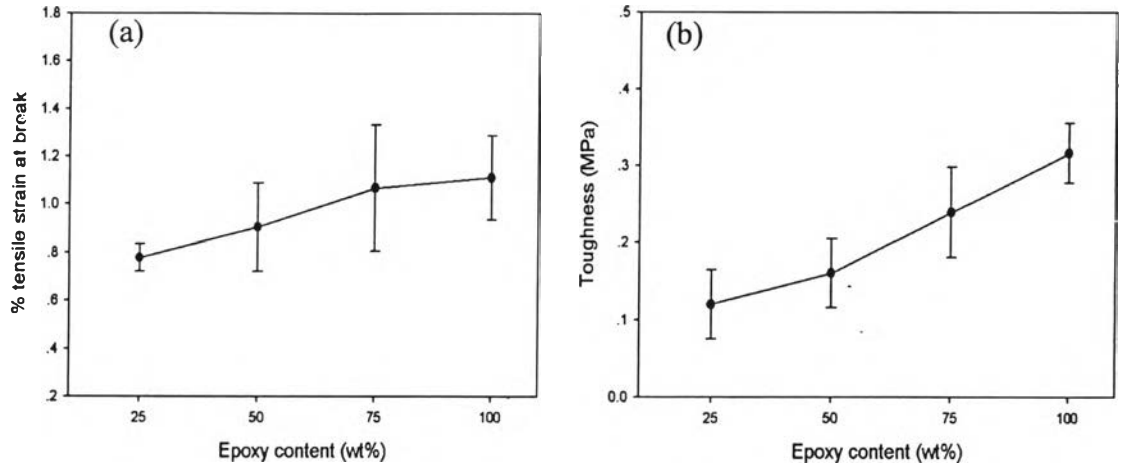

Figure 4.17 Dependence of (a) % tensile strain at break and (b) toughness of sisal-benzoxazine/epoxy composites on the epoxy content in the resin mixture.

Ishida and Allen (1996) showed that increasing the epoxy content of the benzoxazine-epoxy copolymer resulted in a higher crosslink density. High concentration of crosslinks was shown to inhibit the intermolecular packing and enhance network flexibility.

From Figure 4.17 (a) and (b), the tensile strain at break and toughness of the composites were found to increase as epoxy was added. The extensibility of the polymer matrix is due to the decreased intermolecular packing and chain interactions which enhance the ability of segments to flow under load. In summary, the mechanical requirements of a specific application can be processed by varying the epoxy content in the polybenzoxazine-epoxy composites.

4.4.3 Effect of Fiber Surface Modification

Mechanical performance of a fiber reinforced composite primarily depends on three factors: (a) strength and modulus of the fibers, (b) strength and toughness of the matrix, and (c) effectiveness of fiber-matrix bonding in transferring stress across the interface. For a unidirectional composite, longitudinal tensile response is mainly governed by the fiber properties whereas the transverse response

is strongly dependent upon the matrix properties (Cahn, 1993). Thus the effect of surface treatment on longitudinal mechanical properties will be discussed based on the two factors: strength of fibers and interfacial bonding.

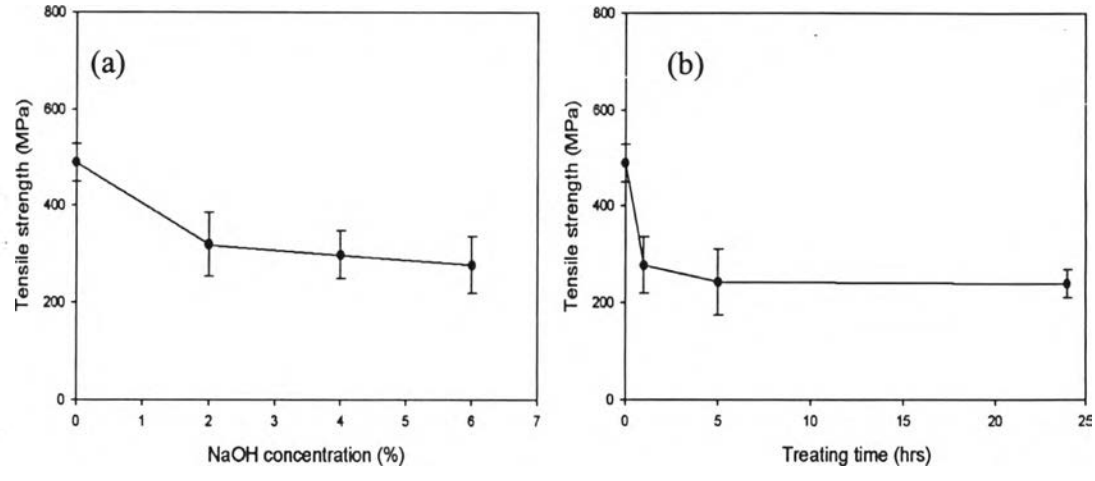

Figure 4.18 Dependence of tensile strength of sisal fibers on (a) NaOH oncentration in 1 h treatment and (b) treating time in 6%NaOH.

The NaOH-treated sisal composites show the tensile strength less than that of the untreated-sisal composites. From the previous study in Section 3.3.1, NaOH treatment partly removes the cementing materials, lignin and hemicellulose, in sisal fibers so this may reduce strength of the fiber. The fiber tensile testing was carried out by varying NaOH concentration and treating time. The results are shown in Figure 4.18. It can be seen that the tensile strength of sisal is reduced by NaOH treatment. The reduction of fiber tensile strength is high initially followed by a gradual reduction at greater NaOH concentration and longer treatment time. Sreekala and Thomas (2003) also observed that the tensile strength of oil palm fibers were reduced after 5%-NaOH treatment for 48 hours. Although the fiber-matrix adhesion may be improved and the stress may be transferred well to the fibers, it cannot compensate for the reduction in fiber strength and, hence, the tensile strength of the composites is not as high as that of the untreated-sisal composites.

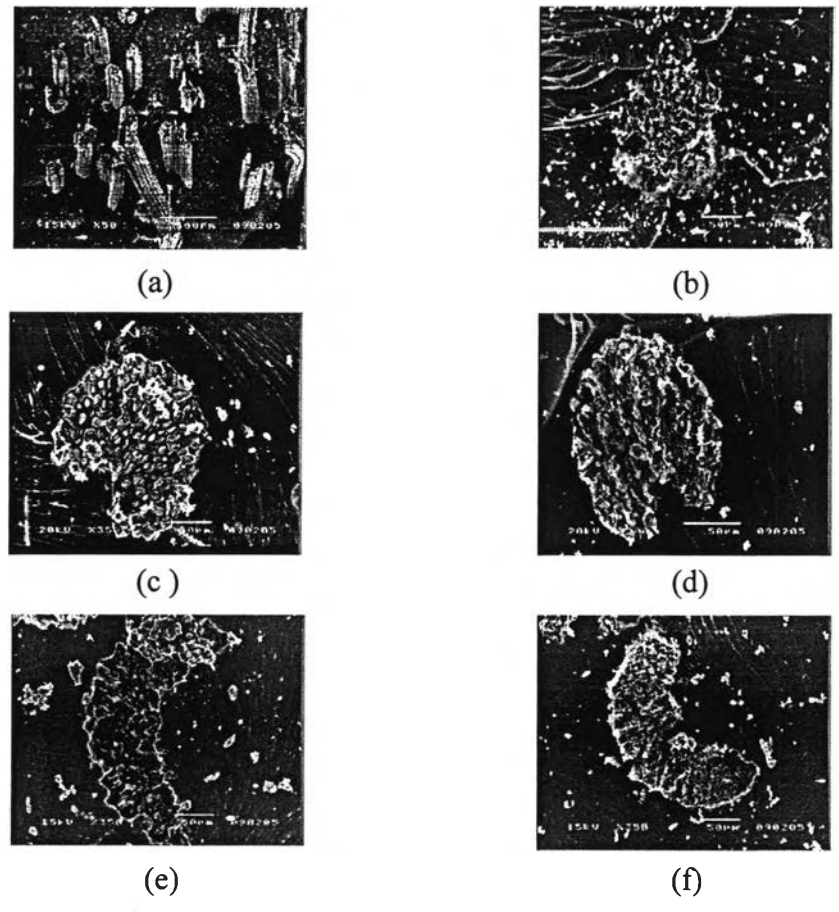

Figure 4.19 SEM micrographs of tensile fracture surface of sisal-benzoxazine/epoxy composites using (a) untreated sisal; (b) NaOH-treated sisal; (c) γ–APS-treated sisal; (d) NaOH/ γ–APS-treated sisal; (e) γ–GPS-treated sisal; and (f) NaOH/ γ–GPS-treated sisal.

However, the tensile modulus of NaOH-treated sisal composites is higher than that of the untreated one. After NaOH treatment, the sisal fiber surface is rougher and static frictional force is increased thus the fiber-matrix adhesion is enhanced by mechanical interlocking. It is believed that the vacancies outside and inside the fiber left by NaOH treatment facilitate penetration of the resin which replaces the removed cementing materials (Rong, 2001). Since the immigrated resin is connected to the bulk matrix forming a network, the higher rigidity of the composite is also reflected on the decrease in its extensibility so the modulus is increased.

The improved adhesion between the treated fibers and polymer matrix can be clearly seen by SEM micrographs of the tensile fracture surface of unidirectional sisal-benzoxazine/epoxy composites as shown in Figure 4.19. With a weak interfacial bond, the fracture is more likely to lead to interfacial debonding and extensive fiber pullout. If bonding is strong, the failure mode is fiber breakage at the fracture point resulting in a fairly smooth surface across the section (Cahn, 1993). For the untreated-sisal composite, the failure mechanism is interface debonding, the composite shows the surface with fiber pulled out from the matrix. On the other hand, fracture of the NaOH-treated fiber occurs at the crack plane in the composite.

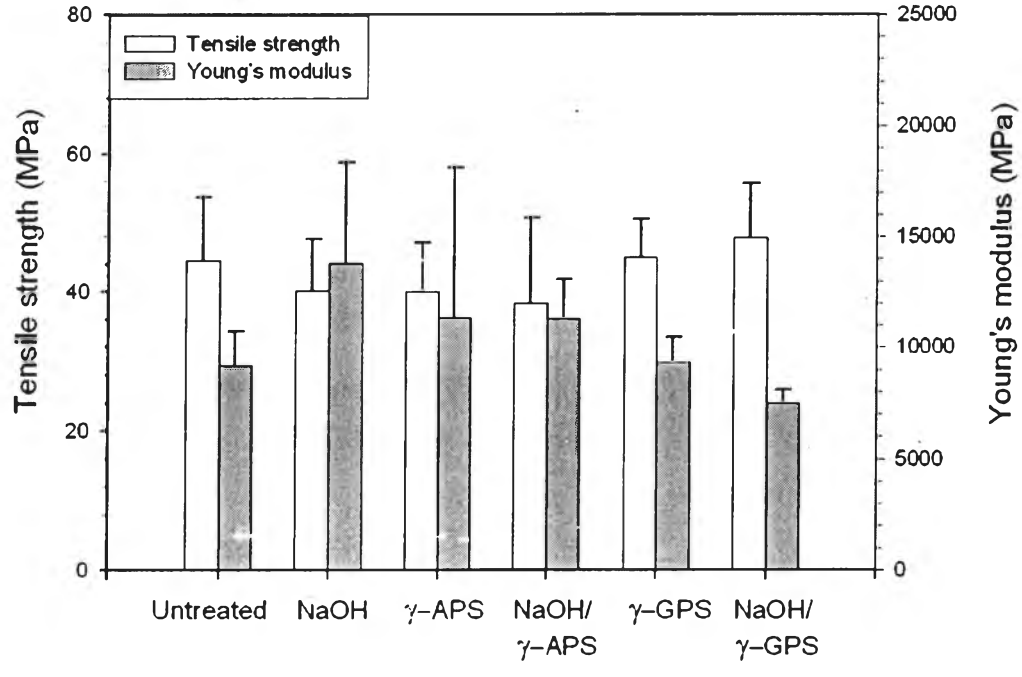

Figure 4.20 Effect of fiber surface modifications on the tensile properties of sisal-benzoxazine/epoxy composites.

The γ–APS-treated sisal composite and the NaOH/ γ–APS-treated sisal composite show similar tensile properties. The tensile strength of these composites is lower than that of the untreated-sisal composite. From Figure 4.20, it can be seen that the tensile strength of γ–APS-treated sisal fiber is reduced due to the fact that the fiber treatment with the amino silane is done in a basic condition (alkoxy

groups of γ–APS are hydrolyzed in water. Thus, the natural pH of the silane solution exceeds 10 (Plueddemann, 1982)) like alkaline treatment so some cementing materials of fibers may be partially removed. The tensile strength of NaOH/ γ–APS-treated sisal fiber is lower than that of sisal fiber treated by only γ–APS. This reduction of fiber tensile strength causes lower composite tensile strength than the untreated one. However, the relatively high modulus of γ–APS-treated sisal composites compared to untreated-sisal composites reveals the less tensile strain at break and the better interfacial interaction, which can be explained as in the case of alkaline treatment. The SEM micrographs of tensile fracture surface give supporting evidence. The SEM results do not show indication of fiber pullout, which indicates good adhesion between matrix and fiber. The improvement of interfacial bonding in the γ–APS-treated sisal composite is the result of hydrogen bonding between amino groups on the γ–APS-treated fiber and hydroxyl groups in the polymer matrix.

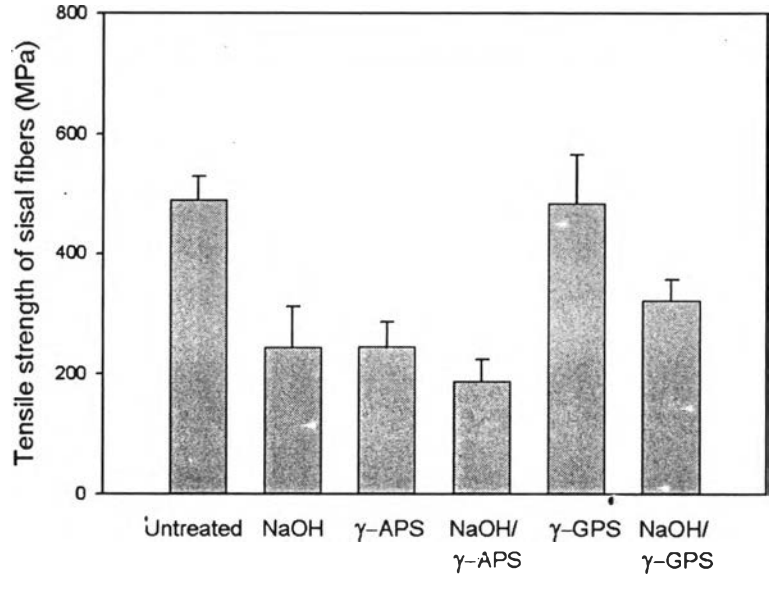

Figure 4.21 Dependence of tensile strength of sisal fibers on surface modifications.

The decreased tensile strength and increased Young's modulus after γ–APS treatment also observed in pineapple leaf fiber-reinforced polyester composites (Devi *et al.*, 1996).

Figure 4.20 shows the tensile properties of the sisal-benzoxazine/epoxy composites with different fiber-surface modifications. γ–GPS-treated sisal composites show tensile strength higher than that of both the untreated and γ–APS-treated sisal composites. Compared to the γ–APS-treated sisal, which forms hydrogen bond to the polymer matrix, the The γ–GPS-treated sisal fiber can bond covalently with the hydroxyl groups of the polymer matrix while minimizing the damage on the fiber during the treatment. Thus in terms of interfacial bonding, the γ–GPS-treated sisal composite is better than the γ–APS-treated sisal composite. In terms of strength of treated fibers, pH of the solution in γ–GPS treatment is about 5.5. Thus, it does not affect the fiber strength as shown in Figure 4.21. Additionally, the hydrogen bonding of the amino group of γ-APS to the fiber surface might reduce the reactivity to the matrix. The results from both factors make the tensile strength of the γ–GPS-treated sisal composite higher than that of the γ–APS-treated sisal composite.

When sisal fiber was first treated with NaOH solution and then by γ–GPS, the tensile strength is improved. It is believed that the γ–GPS can react easily with cellulose microfibrils in the NaOH-treated sisal fibers because alkaline treatment removes some hemicellulose and make cellulose more exposed to fiber surface. Thus NaOH/GPS treatment leads to an interfacial interaction stronger than in the case of γ–GPS or NaOH individual treatment. The highest tensile strength of the NaOH/γ–GPS-treated sisal composite gives supporting evidence.

Compared to tensile properties, Rong *et al.* showed that the flexural failure of the composites depends mainly on fiber/matrix interface rather than fiber strength (Rong, 2001). The results of flexural test in Figure 4.22 agree with the SEM results. In general, flexural strength and flexural modulus are slightly improved by the fiber surface treatments. The NaOH/γ–GPS-treated sisal composite gives the highest flexural properties. This result agrees with the result from the tensile tests which show that NaOH/γ–GPS treatment gives the best interfacial bonding compared to the others in this work.

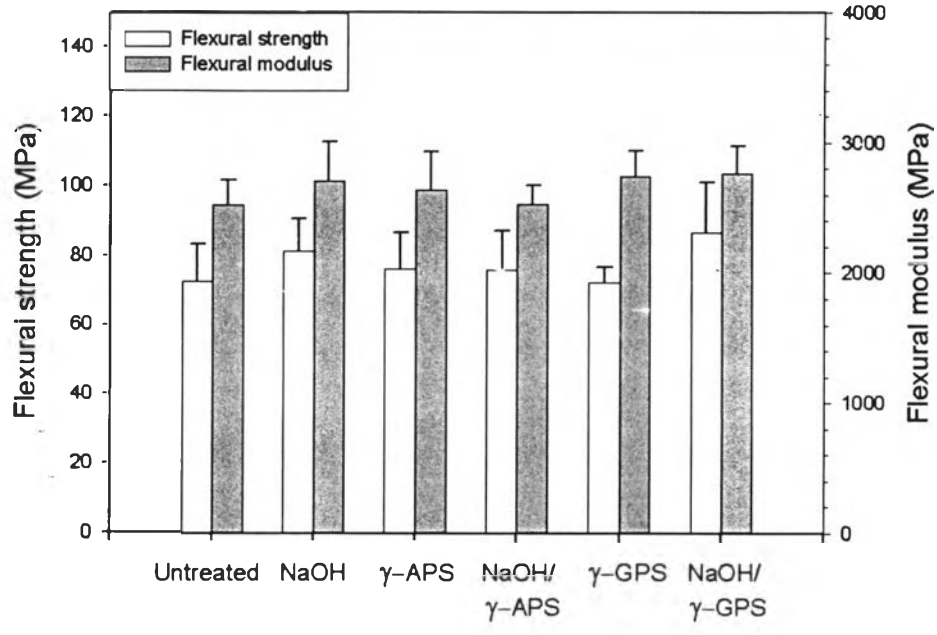

Figure 4.22 Dependence of flexural properties of sisal-benzoxazine/epoxy composites on fiber surface modifications.

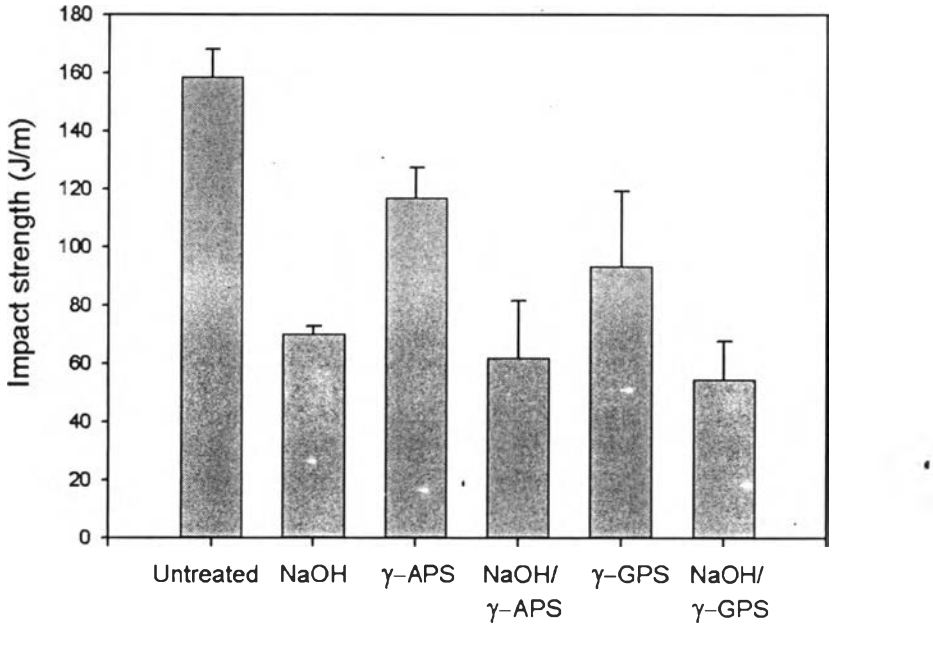

Figure 4.23 Dependence of impact strength of sisal-benzoxazine/epoxy composites on fiber surface modifications.

For the Izod impact test, in all cases of fiber surface treatment, the impact strength of the treated-fiber composites are lower than that of the untreated one. It is important to mention that, in most fiber-reinforced composites, a significant

part of the energy absorption during impact takes place through the fiber pull out process. The low impact strength of treated fiber composites is due to the high bonding of the treated fiber with polymer matrix which results in the fracture of fiber at the crack plane as can be seen from Figure 4.24. The untreated-fiber composite show the impact failure with many fibers pulled out. In contrast, in the case of the treated-fiber composites, more tearing of the fibers could be observed together with a few cavities left by pulled-out fibers.

If the lower impact strength (less energy absorption from fiber pull out process) means better interfacial adhesion, the effect of different surface treatments can be concluded as followings:

i) the NaOH treatment coupled with silane treatment results in better adhesion than the individual silane treatment or NaOH treatment,

ii) the γ–GPS treatment gives better fiber-matrix bonding than the γ–APS treatment. This agrees with the results of tests on tensile strength and flexural strength.

Looking back to the contact angle results, the γ–APS treatment gives higher values of contact angle than the γ–GPS treatment. However, it does not mean that the amino groups of γ–APS could react with polymer matrix better than γ–GPS. Reactivity of the silane with the resin is more significant than wettability of the treated fiber surface. In this case, γ–GPS can form covalent bonds with the resin whereas γ–APS form hydrogen bonds even though the γ–GPS treated fiber show the lower hydrophobic character. However, the contact angle measurement provides useful information on surface modification as described previously.

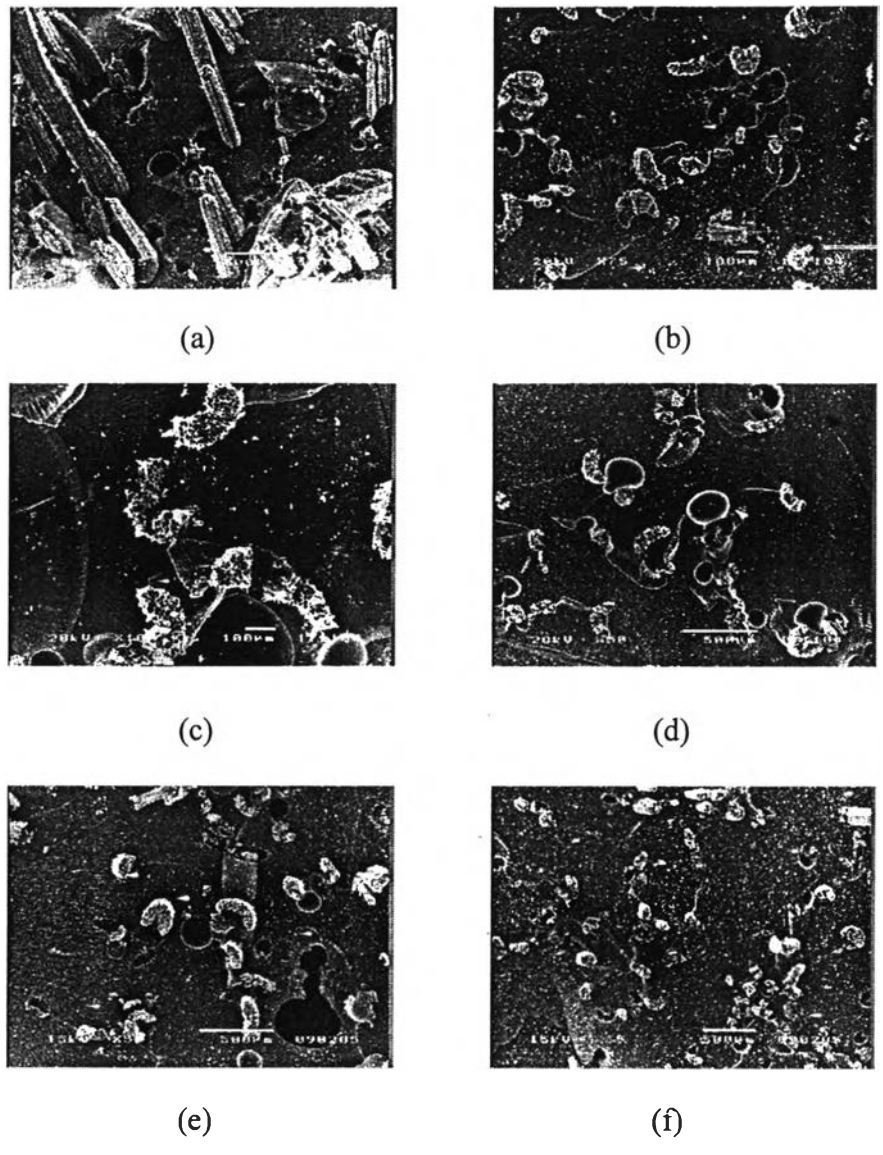

Figure 4.24 SEM micrographs of impact fracture surface of sisal-benzoxazine/ epoxy composites using (a) untreated sisal; (b) NaOH-treated sisal; (c) γ–AFS-treated sisal; (d) NaOH/ γ–APS-treated sisal; (e) γ–GPS-treated sisal; and (f) NaOH/ γ–GPS-treated sisal.